

Accelerated Experimental Investigation of Environmentally Assisted Cracking in AA7085

Jason Rogers[1], Isaac Field[2], Nick Tugwell[2], Maria Salagaras[2], Benjamin Dixon[2]

[1]RMIT University, Melbourne, Australia
[2]Defence Science & Technology Group, Fishermans Bend, Australia

Abstract

Aluminium alloy (AA) 7085 is a modern aerospace grade material that has been found to be susceptible to environmentally assisted cracking (EAC) under certain conditions. This research investigates two methods for accelerating EAC nucleation and growth in AA7085-T7452 test coupons. The objective is to generate EAC cracks in this material that closely resemble real world findings, allowing for investigation of the impact of EAC on component structural integrity, including the potential for fatigue cracks to develop from EAC. Both methods involved pre-conditioning fastener holes in the coupons with a corrosive solution to cause pitting and intergranular corrosion, from which EAC could initiate and grow. Sustained tensile stress was then applied to the pre-conditioned holes in combination with a 70°C and 85% relative humidity environment to promote EAC growth. The pre-conditioning process successfully accelerated EAC initiation and reduced the variability in time to initiation for both test methods. Moreover, the EAC cracking produced away from the pre-conditioned areas near the hole bores closely resembled real-world EAC findings.

Keywords: Corrosion, Aluminium, SCC, EAC, Fatigue

1. Introduction

The susceptibility of aluminium alloy (AA) 7085 to environmentally assisted cracking (EAC) has been the topic of recent research [1-3] due to the emerging usage of AA7085 in modern airframes. EAC includes, but is not limited to, corrosion driven processes such as stress corrosion cracking (SCC), corrosion fatigue and intergranular corrosion (IGC) [4-6]. EAC initiation and growth requires a susceptible material, an environment conducive to corrosion and sustained tensile loading [7, 8]. EAC in AA7085 is associated with macroscopically brittle intergranular crack growth [9], typically growing with minimal corrosive dissolution of material [10]. As a result, EAC growth can degrade structural integrity in the absence of visible corrosion on affected surfaces making it difficult to detect. Thus, a deeper understanding of growth rates and growth mechanisms in AA7085 are crucial to assess the risk of EAC to real world AA7085 components.

The reduction of EAC occurrence was one of the critical considerations during the development of modern high-strength, high-toughness 3rd generation aluminium alloys, such as AA7085 [9]. This goal was motivated by past real world SCC issues observed in first-generation aluminium alloys, including AA7075-T6 and AA7079-T6 [11]. During the development of these alloys, the standard ASTM test for SCC susceptibility using saline alternate immersion testing was employed [10]. The results indicated satisfactory resistance to SCC initiation [12]. However, recent real world EAC findings in these alloys, including AA7085, within a short timeframe suggest that these alloys are susceptible to EAC [13], with more recent evidence suggesting the specific mechanism likely to be SCC [8]. It appears that the ASTM screening tests were insufficient in identifying this susceptibility. Notably, AA7085 has been found to be particularly vulnerable to warm, humid air environments, even in the absence of salinity, which can lead to cracking along grain boundaries without substantial

corrosion on the crack faces [13]. These conditions differ significantly from those used in the standard ASTM screening test.

The limitations of the standard ASTM alternate immersion tests have prompted researchers, including those at Airbus [14], to devise alternative accelerated testing methods to initiate and propagate EAC in AA7085 and other similarly susceptible 3rd generation aluminium alloys under conditions that more accurately simulate those triggering real world EAC. A notable outcome from this research was the recommendation in the European Union Aviation Safety Agency (EASA) safety information bulletin (SIB) [13] to employ conditions of 70°C and 85% relative humidity (RH), with a minimum test duration of 100 days, for meaningful EAC growth [9] to assess EAC susceptibility.

This paper outlines the development of testing methods that expand upon those proposed by previous researchers and recommended by EASA, with the objective of inducing EAC in AA7085-T7452 material that accurately represents real world cracks. The ultimate goal is to use test specimens with such representative cracks to investigate the impact of EAC on the structural integrity of AA7085-T7452 structural components, including the potential for EAC to nucleate fatigue cracks that could sever critical load paths. Given that fastener holes are a common site for EAC to occur, the specimens employed in this study contain holes that simulate those present in real world, structural components. The presence of crevices, moisture retention, exposure of material end grain at the bore, and potential lack of protective coatings make fastener holes particularly susceptible to corrosion. The testing methods described here also encompass the development of techniques to rapidly initiate EAC, thereby reducing the time required to generate representative EAC and minimise the scatter in time needed to develop such cracks. Optical and scanning electron microscope (SEM) assessments show these methods develop intergranular cracking that is representative of real world EAC.

The microstructure of forged AA7085-T7452 exhibits a high degree of anisotropy, characterised by elongated, "pancake-shaped" grains aligned parallel to the L-direction [15]. Consequently, the favoured orientation for EAC growth is parallel to the L-T plane, representing a low-energy pathway [4]. To induce sustained stress at the holes in the coupons, thereby promoting the growth of representative EAC, we developed two alternative methods. The first method involved inserting an interference-fit fastener to impose sustained tensile hoop stresses in the vicinity of the hole, the coupons are then placed in an environmental chamber that maintains a temperature of 70°C and 85% RH. This setup consistently generates growth along the most vulnerable L-T plane.

The second method applies sustained stress at the hole via loading the coupon in a uniaxial test machine and necessitated the design of a custom-built environmental chamber that surrounds the test section of the specimen, ensuring maintenance of 70°C and 85% RH. Although more complex, the second method provides greater flexibility to modify stress, hole conditions and control the direction of loading relative to the local microstructure. While the L-T plane, along which EAC typically grows, tends to be parallel to the primary direction of stresses from in-flight loads, concerns were raised that an unfavourable combination of local sustained stress relative to the local microstructure direction could cause EAC to grow towards the short or transverse directions (Figure 1). This scenario could pose a more significant threat to structural integrity, including the nucleation of fatigue cracks. Our second test setup allows us to test specimens oriented in the L-S, S-L, and T-L directions (Figure 1) to investigate how different combinations of stress direction and local microstructure can generate EAC.

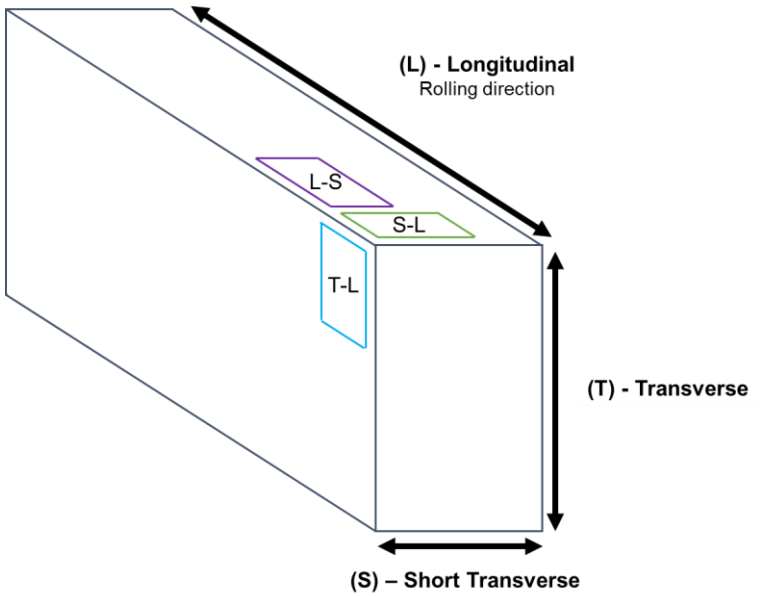


Figure 1: EAC test coupon orientations relative to the original forging direction.

2. Method

2.1. Specimens

Two distinct specimen types were developed for the test method, both made from an AA7085-T7452 hand forging and 5 mm thick. The surfaces were anodised in accordance with MIL-A-8625 type 1C, class 1 sulphuric acid process prior to having their holes machined, replicating a corrosion protection scheme used on some AA7085-T7452 structural components. The unprotected hole bores replicate the conditions in real world structural components and encourage the development of EAC. The dimensions and local microstructure orientation for each specimen type are depicted in Figure 2.

The smaller specimens, displayed in Figure 2a, were used to evaluate the effectiveness of pre-conditioning the specimen holes with a corrosive liquid in accelerating the development of EAC and to investigate the optimal size of fastener and level of interference at the hole for inducing accelerated EAC. The larger specimens were loaded along their longitudinal direction in the uniaxial test machine and typically had an empty 6.35 mm diameter hole.

The objective of this research is to accelerate the generation of real-world-representative EAC in AA7085-T7452 material. All test coupons were subject to a pre-exposure step, where the hole bore region intended for EAC growth was exposed to a corrosive solution for an extended period to facilitate pitting and IGC from which EAC can grow. This greatly reduces the scatter in the initiation of EAC versus real world cracks, as well as reducing the time for it to grow to the required test size. Two loading methods were used to generate EAC, facilitating the three basic requirements for EAC: susceptible material, tensile loading and corrosive environment.

The first loading method uses interference fit fasteners (IFFs) which are inserted into anodised AA7085 test coupons after pre-conditioning. Preliminary test coupons were first used to identify the optimal test parameters before moving to larger coupons which can be subjected to fatigue loading. Once the IFF is pressed into the coupons, they are placed into an environmental chamber set to 70°C & 85% RH until EAC from the hole grows to the desired length.

The second loading method involves an anodised AA7085 test coupon placed in a controlled environment, set to 70°C and 85% RH, whilst being held under a tensile load in-situ. Coupons were machined from a large forging in three orthogonal orientations, S-L, L-S and T-L, however this work presents the results from L-S coupons only, the remaining data will be presented in future work.

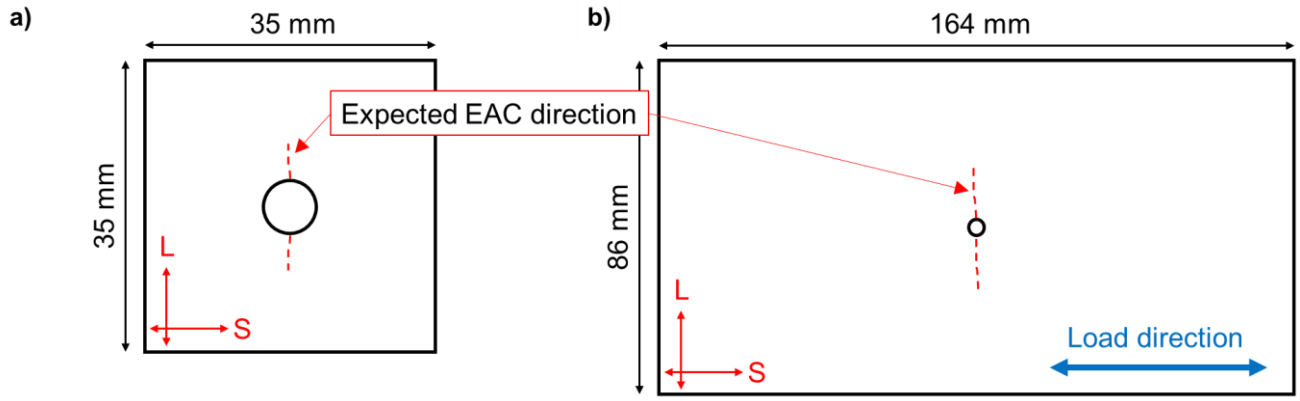


Figure 2: a) Preliminary IFF coupon geometry, hole size is dependent on the designated fastener size and nominal interference level. b) In-situ loading coupon geometry, hole size is dependent on designated fastener size and nominal interference level. Load direction for this coupon is detailed. The expected orientation of EAC in these S-L coupons is depicted in the figure, parallel to the L-T plane.

2.2. Pre-conditioning

With the objective of expediting the initiation phase of EAC, we exposed the bores of specimen holes to a corrosive liquid before subjecting them to sustained tensile stresses within 70°C and 85% RH conditions. The corrosive liquid consisted of potassium persulfate (0.05 M/L) and aluminium chloride (0.033 M/L), with the balance made up of de-ionised water. Hereafter, this solution will be referred to as PP+AC. Initial tests using the PP+AC solution revealed intergranular corrosion (IGC) to a maximum depth of approximately 1 mm and a moderate level of pitting at the hole. Optical and SEM examination of the surfaces corroded by the PP+AC solution for approximately 24 hours showed an excessive level of grain boundary attack versus what had previously been observed for real world cracks (Figure 3). Furthermore, the self-limiting nature of this solution was evident as prolonged exposure did not extend the maximum depth of IGC beyond approximately 1 mm, which is insufficient to replicate the severity of real world EAC that could pose a risk to the integrity of structural components. Nevertheless, we hypothesised that the intergranular attack at the hole bore could establish favourable conditions for the rapid initiation and growth of more representative EAC when exposed to the 70°C and 85% RH conditions used by previous researchers.

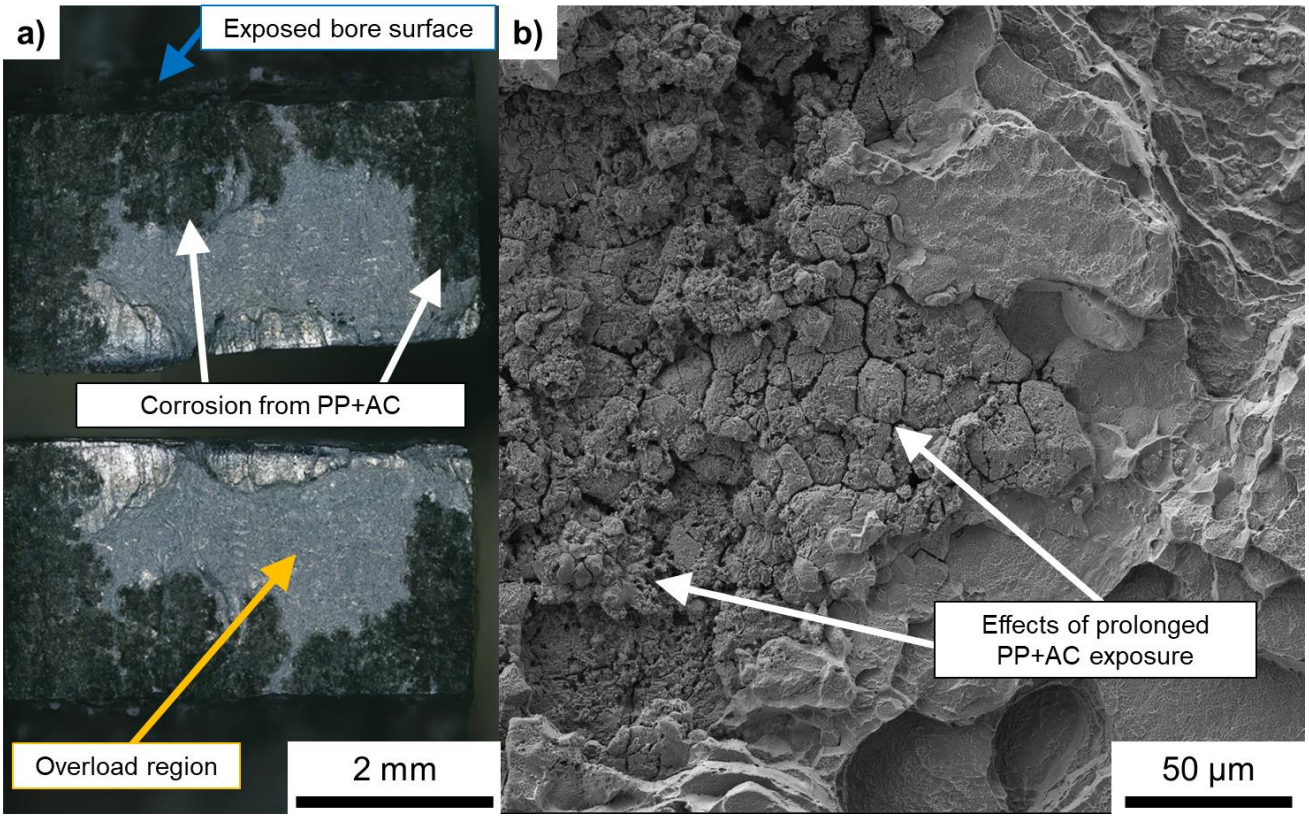


Figure 3: Effect of prolonged exposure to the PP+AC solution for AA7085-T7452. a) Dark regions on this fracture surface are corrosion, comprised of both IGC and pitting. The coupon pictured here was broken open after exposure to PP+AC for approximately 24 hours. b) SEM image showing excessive intergranular attack versus real world EAC on the fracture surface of the same AA7085-T7452 coupon.

For pre-conditioning, the hole in each specimen was exposed to the PP+AC solution using temporary reservoirs affixed to the coupon with sealant (Figure 4). During our trials, we tested various exposure times to the PP + AC solution, specifically 2, 8, and 24 hours, with the goal of determining the optimal exposure time to accelerate EAC development while producing a crack surface that mimics the morphology of real-world cracks and limits severe intergranular attack to the area surrounding the hole bore. Following the prescribed exposure time, the hole bores were rinsed with de-ionised water in an ultrasonic cleaner, followed by final cleaning with ethanol to remove the PP + AC solution and minimise its influence on EAC growth away from the hole bore.

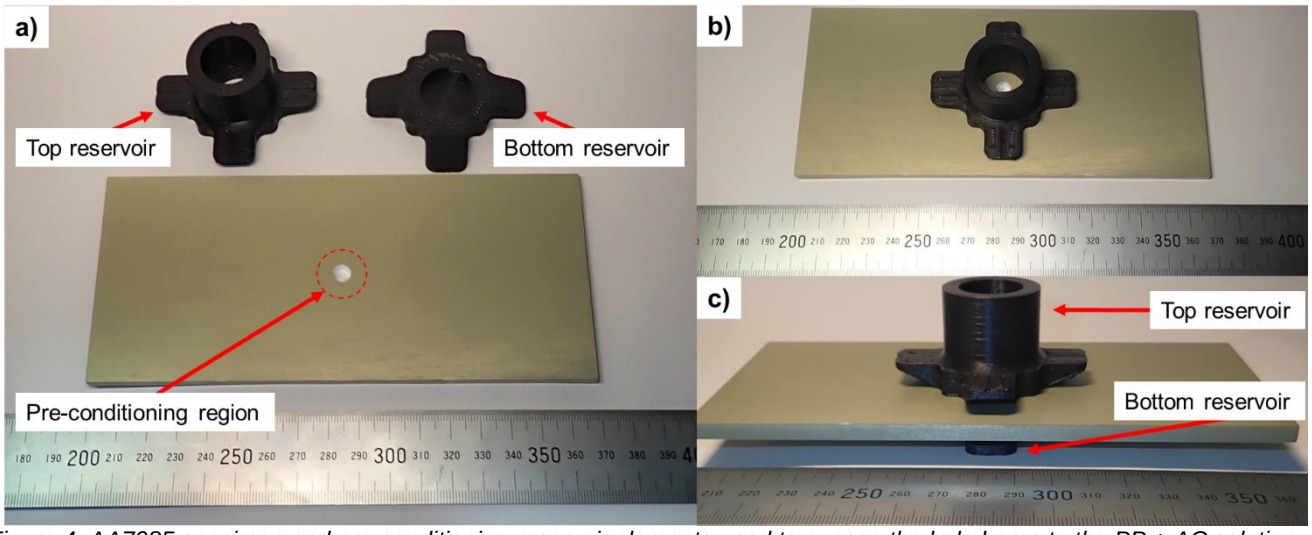


Figure 4: AA7085 specimen and pre-conditioning reservoir elements used to expose the hole bores to the PP + AC solution used during pre-conditioning.

2.3. Interference fit fastener coupons

The first loading method employed to generate EAC in AA7085-T7452 used IFFs to create a sustained tensile stress field around a fastener hole in the square AA7085 coupons, as depicted in Figure 5. The fasteners were Hi-loks™, made from Ti-6Al-4V alloy and had a HI-KOTE™ aluminium pigmented coating, which likely reduced galvanic coupling between the titanium fastener and AA7085 specimen. Ti-6Al-4V Hi-lok™ fasteners are frequently used in aluminium alloy structural components, and the higher stiffness of this material compared to AA7085 facilitates the imposition of tensile hoop stress at the hole when interference fit occurs. As detailed in Table 1, we tested various combinations of hole size and interference level to establish the optimal combination that would efficiently produce EAC long enough to be representative of the most severe real world findings within a minimal time frame. Holes were drilled precisely, and their diameters were measured, while the fasteners were also measured to ensure the achieved level of interference was close to the targeted value.

Table 1: Test matrix to determine the optimal fastener size (in), interference level (%) and PP+AC pre-exposure time (hours) for real-world-representative EAC growth in AA7085 coupons.

		Nominal interference level			
		0.5%	1.0%	1.5%	2.0%
PP+AC pre-exposure time	2 hours	1/4"	3/16”	5/32”	1/4"
	8 hours	1/4" & 3/16”	3/16” & 5/32”	5/32”	1/4"
	24 hours	1/4"	3/16” & 5/32”	5/32”	3/16”

After pre-exposure, cleaning and inserting the IFF using a hydraulic press, the IFF coupons were placed into an environmental chamber (Vötsch C340) set at 70°C and 85% relative humidity (RH) for approximately 60 days. To avoid condensation on the coupons, the chamber was held at 70°C and 10% RH for 6 hours before ramping the humidity up to 85% RH.

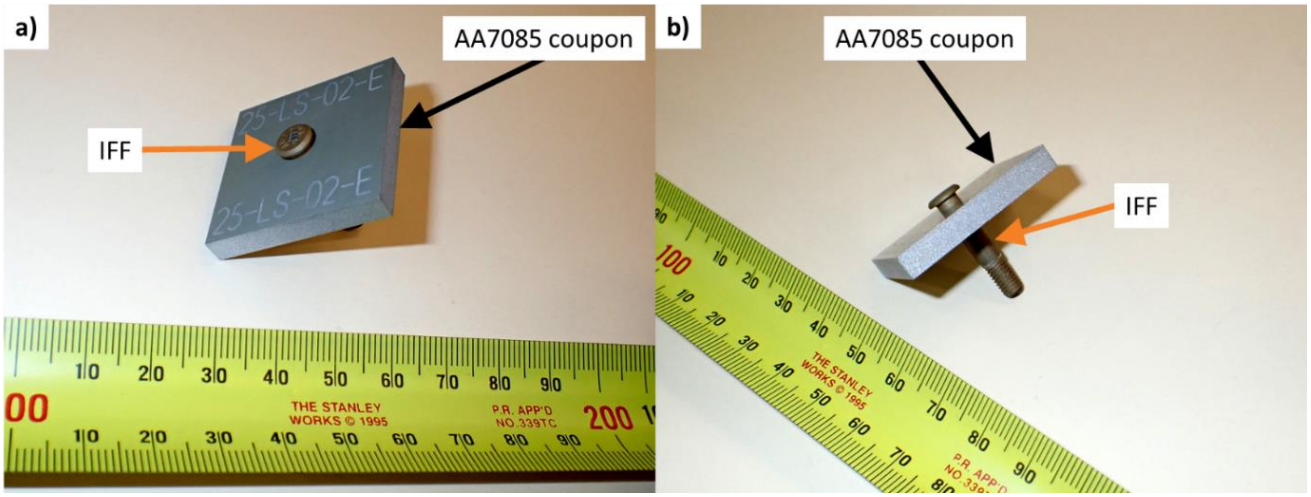


Figure 5: A square AA7085 coupon with IFF installed. The major faces of the coupon are anodised.

2.4. Applying sustained stress via a uniaxial electromechanical test machine

After preconditioning with the PP + AC solution, the longer AA7085 test coupons (Figure 2b), were subjected to sustained stresses at their holes using an electromechanical universal test machine (Instron equipped with a 100kN load cell). To maintain the required 70°C and 85% RH conditions necessary for growing real world-representative EAC, the test section of the coupon, including the hole, was housed within an environmental sub-chamber (Figure 6d). This chamber was insulated and sealed to minimise heat loss and was connected to a Vötsch C4-340 commercial environmental chamber via insulated ducting (Figure 7). A fan built into the door of the commercial chamber was used to circulate moist hot air from the commercial chamber through to the sub-chamber.

Bespoke grip extension fixtures were designed to ensure that the Instron machine grips remained outside the sub-chamber, preventing corrosion (Figure 6b). Additionally, the connections between the

grip extension fittings and the specimens were enclosed within sealed isolation boxes to prevent the ingress of hot humid air, reducing the potential for corrosion at this interface (Figure 6c). The test coupons were loaded to a nominal gross section stress of 115 MPa, which is equivalent to approximately 345 MPa at the edge of the hole, representing around 75% of the yield stress.

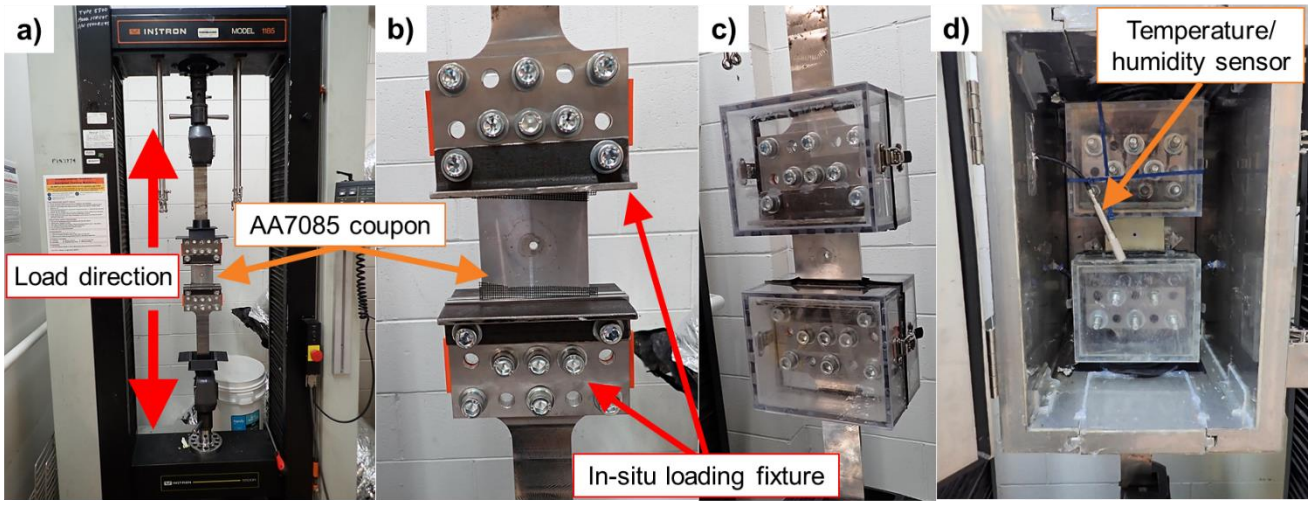


Figure 6: AA7085 EAC coupon mounted in the electromechanical Instron test machine using b) in-situ loading fixtures and c) isolation boxes to avoid corrosion at this interface. d) Coupon mounted inside the sub-chamber with the temperature/humidity sensor in place.

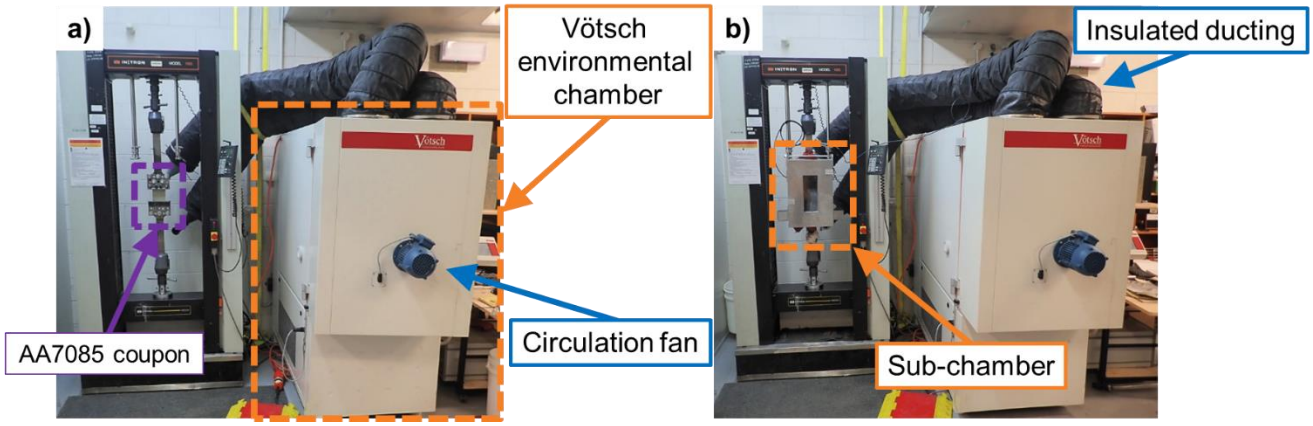


Figure 7: Environmental sub-chamber static testing setup a) without the sub-chamber installed and b) with the sub chamber installed.

A dual temperature and humidity sensor was installed in both chambers, shown in Figure 6d. Data recorded using these sensors revealed a significant drop in temperature (>10°C) and an increase in humidity (>30% RH) in the sub-chamber compared to the commercial chamber. Nonetheless, the temperature and humidity in the commercial chamber were adjusted appropriately to sustain conditions in the sub-chamber within 5% of the nominal 70°C and 85% RH, as shown by the temperature and RH traces obtained during a calibration test cycle in Figure 8a and b respectively. To avoid condensation during EAC testing, humidity was ramped up after the target temperature in the main chamber was sustained for at least 2 hours.

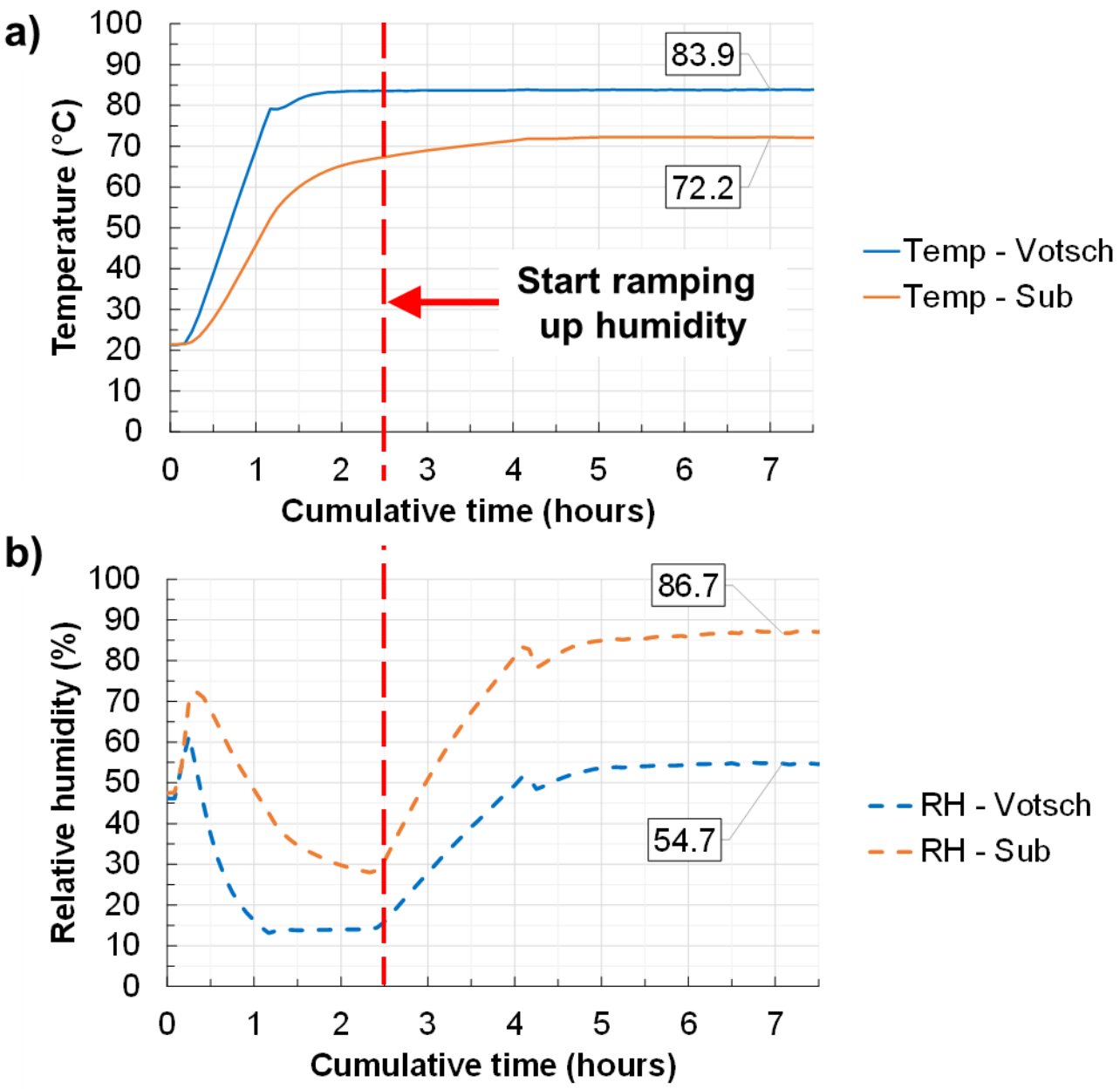


Figure 8: a) Temperature data and b) relative humidity data obtained from temperature/humidity sensors placed in the main (Votsch) and sub chamber during a calibration test cycle. By adjusting the temperature and humidity in the main chamber we could sustain conditions close to the desired 70°C and 85% RH in the sub chamber where EAC was grown.

3. Results

3.1. Pre-conditioning

Pre-conditioning using the PP+AC solution was found to be effective in producing IGC and surface corrosion pitting in AA7085-T7452 material. These corrosion features served as favourable initiation sites for EAC as shown in the optical microscope image in Figure 9. This image (Figure 9) shows an AA7085-T7452 coupon that was broken open after EAC testing using the in-situ loading fixture. This coupon was subjected to 8 hours pre-conditioning using the PP+AC solution. The dark regions near the hole bore in Figure 9 are IGC and surface pitting produced as a result of pre-conditioning. The lighter regions extending from the dark corrosion regions are EAC, which is distinctively intergranular, but largely free from corrosion product. It is acknowledged that pre-conditioning is not representative of the effects of typical environmental exposure. However, it has successfully been used here to generate EAC away from the bore of the hole that is representative of real world cracks and reduce the variability associated with time to initiation.

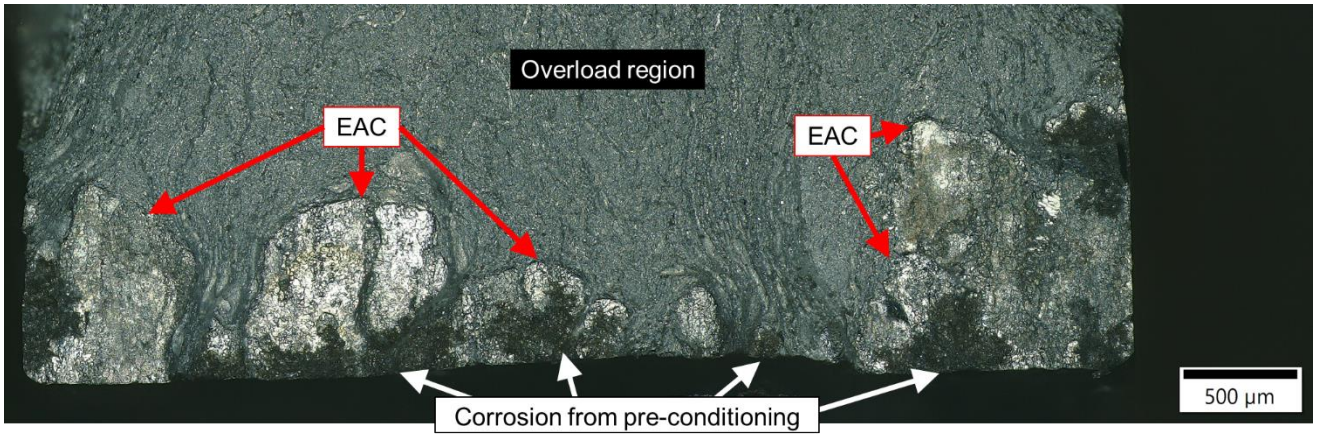


Figure 9: Fracture surface of an AA7085-T7452 coupon that was broken open after testing using the in-situ loading fixture. EAC is generated from IGC that is produced by the PP+AC solution in AA7085-T7452. This coupon was pre-conditioned for 8 hours using the PP+AC solution.

3.2. IFF coupons

EAC cracks were successfully generated in AA7085 coupons with IFF after being exposed to 70°C and 85% RH for approximately 8 weeks, these cracks were visible from the surface of the coupons as shown in Figure 10a. Breaking the coupons open revealed the true scale of EAC as shown in Figure 10b, where EAC has grown from the bore of the IFF hole, parallel to the coupon longitudinal grain orientation. EAC cracks bear the distinct intergranular appearance expected for real world EAC in AA7085-T7452 as seen in Figure 10c and d.

To evaluate the effectiveness of different combinations of pre-conditioning time, interference level, and fastener size, we measured the lengths of the largest EAC cracks in each coupon using an optical microscope following destructive inspection. The maximum EAC crack length for all coupons tested is plotted in Figure 11, and the longest observed EAC crack in AA7085 IFF coupons was approximately 5.15 mm long.

Upon close examination after destructive inspection, we found that EAC grew from the pits and IGC caused by pre-conditioning for all coupons except two, demonstrating the effectiveness of the pre-conditioning stage. However, there was scatter in the crack lengths achieved with any combination of conditions, as shown in Figure 11.

We found that 2 hours of pre-conditioning was insufficient to effectively initiate EAC, while there was minimal difference in maximum crack length achieved using 8 hours PP+AC pre-exposure time compared to 24 hours pre-exposure time. Furthermore, after 24 hours of PP+AC pre-exposure, excessive IGC was observed on the fracture surface close to the hole bore and the crack morphology appeared to deviate from real world findings. Therefore, we have decided that future experiments will

be conducted using an 8-hour PP+AC pre-exposure time.

Interference levels of 1% and above resulted in similar crack length ranges by the end of the testing period. Therefore, we have chosen to use 1.25% interference in future tests.

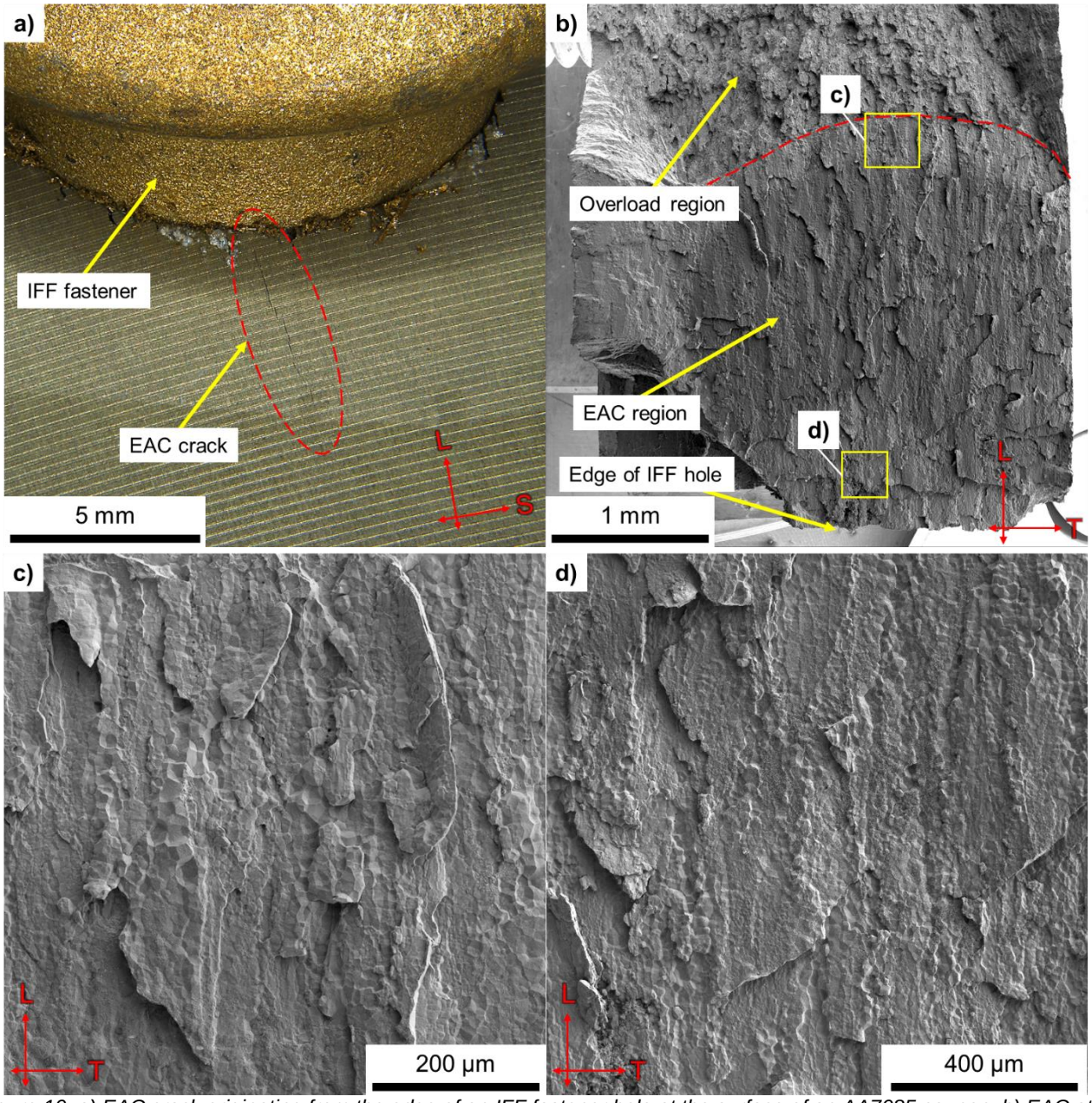


Figure 10: a) EAC crack originating from the edge of an IFF fastener hole at the surface of an AA7085 coupon. b) EAC at a fracture surface after a coupon has been broken open. The maximum crack length from the hole bore is 4.22 mm. c) High magnification SEM image of the EAC crack's surface at the region captured at the location indicated in b) showing a distinctive intergranular fracture surface representative of real world EAC findings. d) Another high magnification SEM image of the crack surface at a location indicated in b). The microstructure grain orientation is indicated in all images.

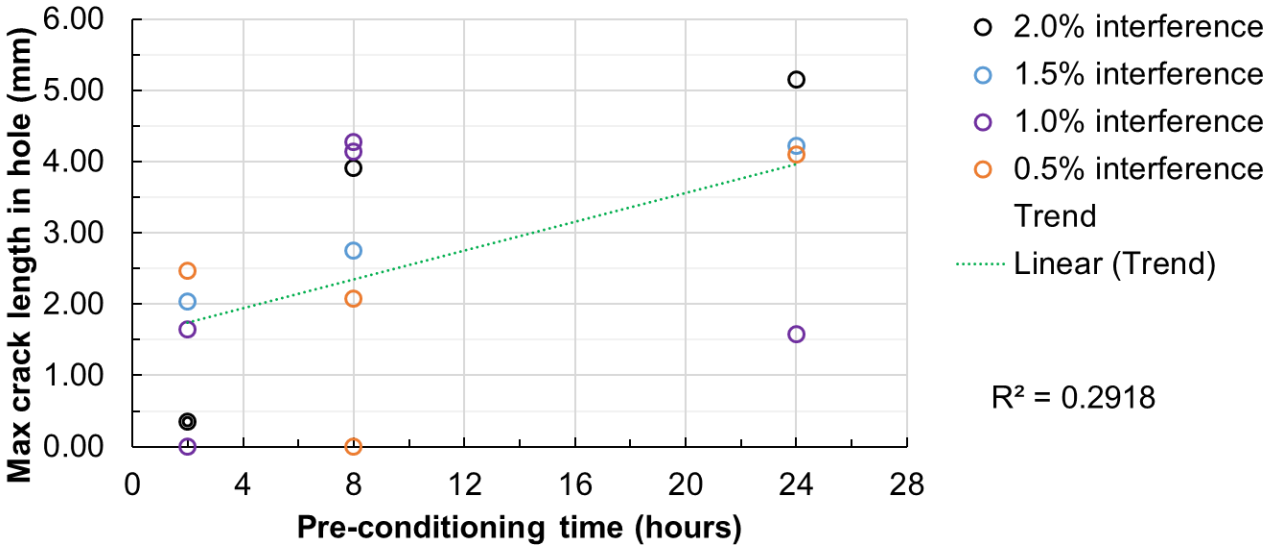


Figure 11: The results of the preliminary IFF testing with pre-conditioning time plotted against the maximum EAC crack length from the hole. The crack length measurements were taken after breaking open the holes to reveal the surfaces of the largest cracks.

3.3. EAC testing with in-situ loading fixture

EAC was successfully generated in an AA7085 coupon using the in-situ loading fixture after approximately 22 days at 70°C and 85% RH. The coupon was then subjected to variable amplitude spectrum fatigue loading until failure to reveal the EAC fracture surface (Figure 12). Marker bands (MBs) were incorporated in the fatigue loading spectrum to make markings on the fatigue crack surface that facilitate the measurement of fatigue crack growth rates. The first MB aided the identification of the fatigue crack nucleation point at the edge of the EAC adjacent to the hole bore.

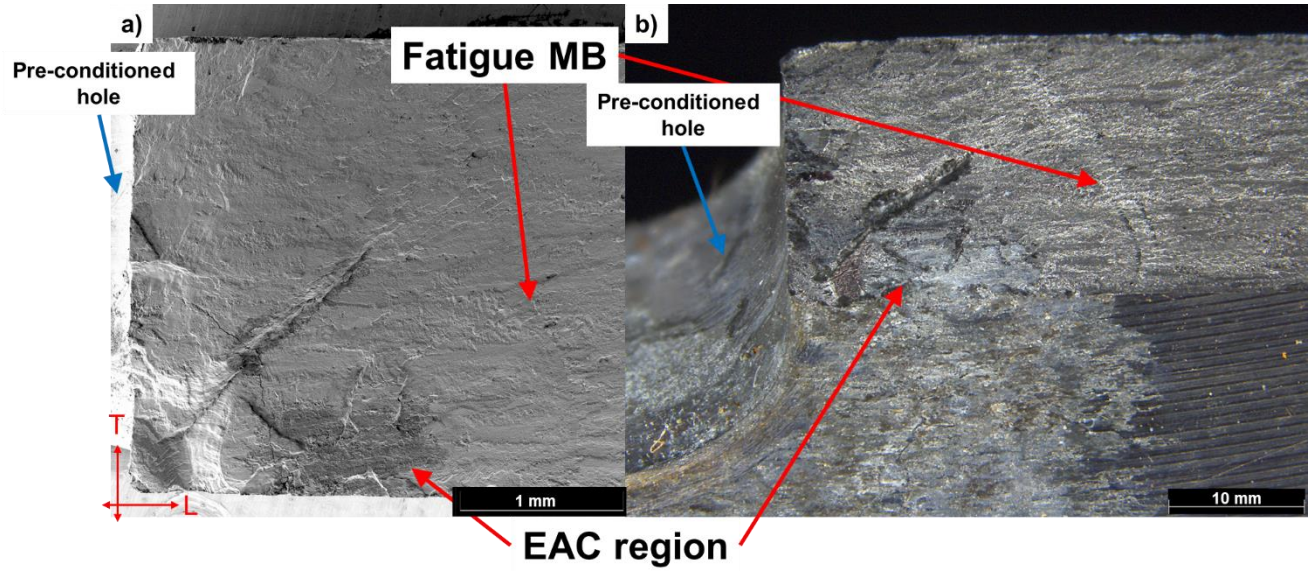


Figure 12: The fracture surface of an AA7085 test coupon imaged after fatigue failure, imaged using an a) SEM and b) optical microscope.

The maximum depth of the EAC region at the coupon surface, adjacent to the hole (EAC region in Figure 13), was approximately 2 mm. When examined using an SEM, a clear demarcation was observed between EAC growth and fatigue crack growth (Figure 13). The EAC region here resembled the EAC region created via the IFF-based tests and exhibited a typical intergranular growth, while the fatigue region displayed transgranular growth, with river patterns and progression markings (including MBs) that are characteristic of fatigue crack growth. This initial test indicated that real world representative EAC readily initiates fatigue cracking if it is favourably oriented relative to the fatigue loading.

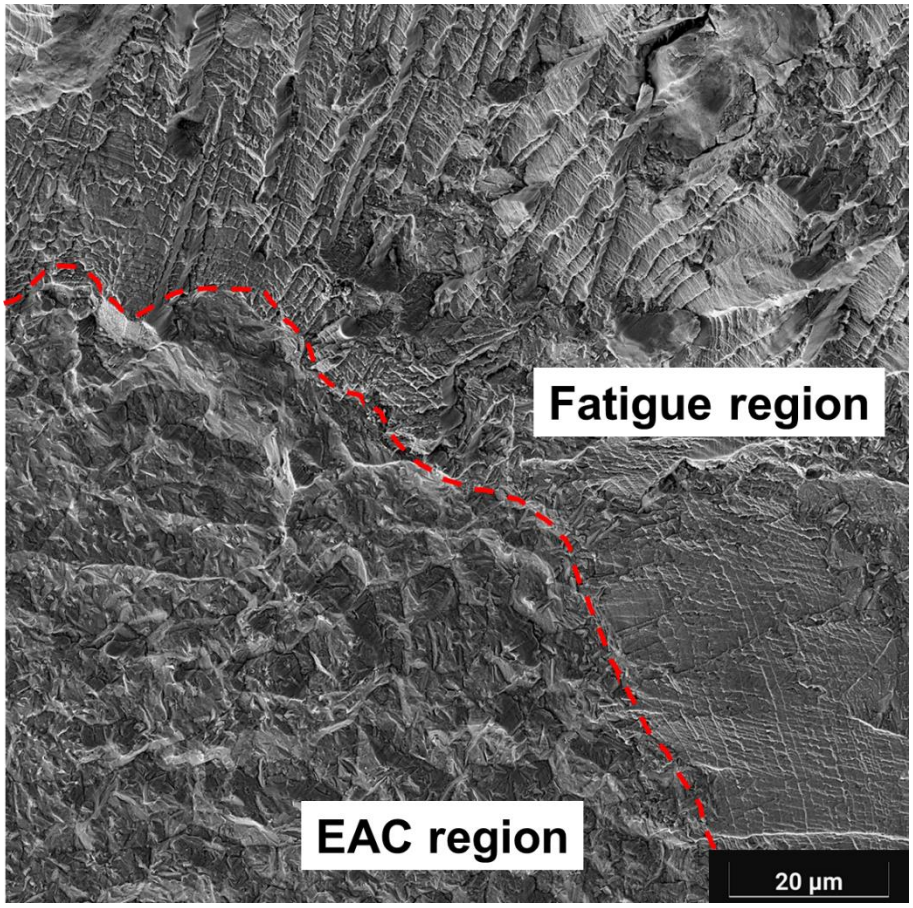


Figure 13: SEM image highlighting the interface between the EAC region and subsequent fatigue crack growth for an AA7085 coupon that was held in 70°C and 85% RH conditions, then fatigue tested until failure.

4. Discussion

Pre-conditioning of coupons proved to be an effective method for generating real world representative EAC in AA7085. The PP+AC solution resulted in pitting and IGC with excessive grain boundary attack, which differed from real-world EAC, as shown in Figure 9. However, with sufficient time, sustained tensile stresses, and 70°C and 85% RH conditions, EAC with a fracture surface largely free of visible corrosion, which is characteristic of past real world findings, will grow away from the PP + AC affected region (Figure 10). Therefore, we are able to produce EAC where the majority of the fracture surface is representative of real-world findings, while crucially, the EAC crack tip, which is critical for fatigue crack nucleation, is considered representative.

The IFF-based method for generating EAC is efficient, as multiple test coupons can be tested in parallel, provided the environmental chamber is large enough. After approximately 60 days, the maximum EAC crack length achieved using this method was 5.15 mm. We are currently investigating whether holes need to be oversized after the EAC growth stage to eliminate the effects of cold work from the interference fit fasteners, which may influence subsequent fatigue crack growth rates.

The stress direction from IFF is nominally uniform around the circumference of the fastener hole, which means that the stress direction cannot be controlled. All EAC growth observed in IFF coupons was parallel to the L-T plane, which is the preferred direction for EAC growth. In contrast, the in-situ loading setup allows for control over the direction of the loading relative to the microstructural grain direction, enabling the potential growth of EAC on planes other than L-T. Although EAC will grow more slowly on such planes, they could cause cracks that are more likely to generate fatigue cracks in typical stress hot spots of structural components. The stress intensity factor for the in-situ loading setup will also increase more as the EAC cracks grow away from the hole than in the IFF-based tests. Previous studies have indicated that prior to cracking, the material immediately surrounding the IFF experiences a compressive stress, which transitions to tensile stress further away from the fastener

[16, 17].

The in-situ setup allows for the comparison of the effects of various hole and fastener coatings on EAC versus bare AA7085 and Ti-6Al-4V, as well as the impact of corrosion prevention compound (CPC) application. Additionally, it facilitates the estimation of EAC crack growth rates utilising the Direct Current Potential Drop (DCPD) method [18]. On the other hand, the IFF-based method is better suited for producing cracks primarily in the L direction of L-S oriented coupons like those depicted in Figure 2b, which can be fatigue tested in a uniaxial test machine. This orientation of EAC cracks, predominantly parallel to the local fatigue loading direction, is frequently observed for real world EAC findings.

5. Conclusions

This research investigates two methods for accelerated environmentally assisted cracking (EAC) nucleation and growth in AA7085-T7452 test coupons. The goal is to generate EAC cracks in this material that accurately represent real-world findings, enabling investigation of the effects of EAC on the structural integrity of components, including the potential for fatigue cracks growing from them. EAC initiation was accelerated by pre-conditioning the fastener holes in AA7085-T7452 test coupons with a corrosive solution containing potassium persulfate and aluminium chloride. This process generates pitting and intergranular attack, from which real-world representative EAC cracks can initiate and grow. All EAC testing was conducted at 70°C and 85% RH, as recommended in EASA SIB 2018-04R2 [13], to promote faster EAC growth rates.

The first accelerated method uses IFFs in the pre-conditioned holes of AA7085-T7452 coupons to apply sustained tensile stress and the coupons are exposed to 70°C and 85% RH within an environmental chamber to promote accelerated EAC growth. After approximately 60 days, this method successfully generated EAC in most coupons, with a maximum EAC length from the hole of 5.15 mm. The second method applies a tensile load to pre-conditioned coupons via a uniaxial test machine, with an environmental chamber surrounding the coupon in-situ, maintaining the required 70°C and 85% RH environment for accelerated EAC growth. The initial trial of this method generated EAC to a depth of approximately 2 mm after 22 days. Both methods have proven successful in rapidly initiating EAC and reducing variability in time to initiation. Microscopic examination of the surfaces of the EAC cracks generated via these two methods indicates that, away from the pre-conditioning affected areas near the hole, the EAC closely resembles real-world cracks. Both methods offer distinct advantages for investigating different aspects of real world EAC cracks. This includes studying how load direction influences EAC growth direction, the effect of load magnitude, and the applicability of advanced test analysis methods.

6. Contact Author Email Address

jason.rogers2@rmit.edu.au

7. Copyright Statement

The authors confirm that they, and/or their company or organization, hold copyright on all of the original material included in this paper. The authors also confirm that they have obtained permission, from the copyright holder of any third party material included in this paper, to publish it as part of their paper. The authors confirm that they give permission, or have obtained permission from the copyright holder of this paper, for the publication and distribution of this paper as part of the ICAS proceedings or as individual off-prints from the proceedings.

References

1. Kairy, S.K., et al., *The role of microstructure and microchemistry on intergranular corrosion of aluminium alloy AA7085-T7452.* Corrosion Science, 2018. **143**: p. 414-427.
2. Prabhu, T.R., *An overview of high-performance aircraft structural Al alloy-AA7085.* Acta Metallurgica Sinica (English Letters), 2015. **28**(7): p. 909-921.
3. Burnett, T.L., et al., *Mechanisms of environmentally induced crack initiation in humid air for*

new-generation Al-Zn-Mg-Cu alloys. Corrosion, 2023. **79**(8): p. 831-849.
4. Euesden, R.T., et al., *Direct comparison of the environmentally induced cracking resistance of 2nd and 3rd generation alloys, AA7050-T7651 and AA7085-T7651.* Materials & Design, 2025. **253**: p. 113867.
5. López Freixes, M., et al., *Revisiting stress-corrosion cracking and hydrogen embrittlement in 7xxx-Al alloys at the near-atomic-scale.* Nature communications, 2022. **13**(1): p. 4290.
6. Lynch, S., *Mechanisms of stress-corrosion cracking and liquid-metal embrittlement in Al-Zn-Mg bicrystals.* Journal of materials science, 1985. **20**(9): p. 3329-3338.
7. Schwarzenböck, E., et al., *Crack initiation of an industrial 7XXX aluminum alloy in humid air analyzed via slow strain rate testing and constant displacement testing.* Materials Science and Engineering: A, 2021. **804**: p. 140776.
8. Schwarzenböck, E., et al., *Environmental cracking performance of new generation thick plate 7000-T7x series alloys in humid air.* Corrosion Science, 2020. **171**: p. 108701.
9. Free, B., et al., *Measurement of atmospheric corrosion fatigue crack growth rates on AA7085-T7451.* International Journal of Fatigue, 2023. **167**: p. 107368.
10. Gangloff, R.P., *Hydrogen assisted cracking of high strength alloys.* 2003.
11. Holroyd, N.H., et al., *Environment-induced cracking of high-strength Al-Zn-Mg-Cu aluminum alloys: past, present, and future.* Corrosion, 2023. **79**(1): p. 48-71.
12. Aboura, Y., et al., *Understanding the environmentally assisted cracking (EAC) initiation and propagation of new generation 7xxx alloys using slow strain rate testing.* Corrosion Science, 2022. **199**: p. 110161.
13. (EASA), E.U.A.S.A., *2018-04R2 : Environmentally Assisted Cracking in certain Aluminium Alloys*. 2021.
14. Donne, C.D. *Structural Integrity - The Journey Towards Zero Emission Commercial Aircraft*. in *International Committee on Aeronautical Fatigue*. Delft.
15. Srivastava, J., et al., *The influence of partially recrystallized grain structures on hydrogen-environmentally induced cracking (H-EIC) behavior of AA7085 alloy in humid air.* Corrosion Science, 2025: p. 113199.
16. Duprat, D., et al., *Fatigue life prediction of interference fit fastener and cold worked holes.* International Journal of Fatigue, 1996. **18**(8): p. 515-521.
17. Zeng, C., W. Tian, and W.H. Liao, *The effect of residual stress due to interference fit on the fatigue behavior of a fastener hole with edge cracks.* Engineering Failure Analysis, 2016. **66**: p. 72-87.
18. Černý, I., *The use of DCPD method for measurement of growth of cracks in large components at normal and elevated temperatures.* Engineering Fracture Mechanics, 2004. **71**(4-6): p. 837-848.